Amara Zenati et al.

Corrosion study of C-Mn steel type API 5L X60 in simulated soil solution environment and inhibitive effect

A. Amara Zenati[1], A. Benmoussat[1,2]∗,O. Benali,[1,3]

[1] *Corrosion Equip of LAEPO Research Laboratory - Tlemcen University -Algeria*
[2] *Faculty of technology- Chetouan University Pole -Tlemcen University - Algeria*
[3] *Faculty of Science and Technology- Saïda university- Algeria*

Abstract

Buried steels in gas transmission pipelines, are solicited by soil corrosion when the protection is missed. The corrosion behavior is estimated by means of potentiodynamic polarization and electrochemical impedance spectroscopy (EIS) with and without the corrosion inhibitors containing polyphosphates ions. Appropriate models for corrosion parameters are used to fit the experimental data and extract the parameters which characterize the corrosion process. The corrosion rates were studied in different concentrations (10^{-3}, 10^{-2}, 10^{-1} and 5.10^{-1} M) of corrosion inhibitors at different near neutral pH values (5.0, 6.5 and 8.5). Results showed the bare steels sensitivity to corrosion and by increasing the temperature, the polarization resistance decreases and the corrosion speed increases as well as the densities of corrosion current I_{Corr}. Corrosion inhibitors tests showed a variation in inhibition performance with varying concentration, temperature and immersion time. Langmuir model have been tested to describe the adsorption behaviour of inhibitor on the steel surface for the temperature range. Some thermodynamic functions of dissolution and adsorption have been determined.

Keywords: C-Mn steels – simulating soil solution - adsorption mechanism- interface

Introduction

Corrosion steels phenomenon in buried structures such as a gas transmission pipelines is the main problems in oil industry. C-Mn Steels of API 5L X60 are protected from the external soil corrosion by a bituminous coating whose action is coupled with a cathodic protection system (minimum potential specified -850 mV versus (Cu / CuSO$_4$), which aims to maintain steel in its protection field and thus, to avoid any risk of corrosion during a possible rupture of the coating. However, the expertise studies carried out on GZ1 line [1] after forty years of service revealed many types of failures such as: pitting corrosion, canalization perforation, coating failure, cracking and biocorrosion... These failings occurred in consequence of bare steel interaction in the aggressive area soil like montmorillonite clay soils or saline underground waters subsoil. Considering the recidivist corrosion type in these sites, we have proposed to complete the protection of steel by addition of inhibitors. Steel corrosion phenomena in underground conditions are still unclear, because soil is a complex environment material. Chemical composition is a key to understanding how a soil can influence the corrosion. It is necessary to examine every particular site to explain the corrosion mechanisms models resulting from the steel interaction with the soil environment which depends of numerous factors such as soil nature, moisture content, soil resistivity soil pH, and oxidation – reduction potential…The objective is to bring a better comprehension of corrosion damage mechanisms to reduce steel failures in service. Appropriate models for corrosion parameters such as corrosion current density (I_{corr}), corrosion potential (E_{corr}), polarization resistance (R_p), soil resistivity (ρ) are used to fit the experimental data and extract the parameters which characterize the corrosion process. Potentiodynamic polarisation and electrochemical impedance spectroscopy (EIS) were carried out.

Corrosion phenomena are studied in artificial solutions. The effect of temperature on the values of the electrochemical parameters characterizing the systems has been recorded by polarisation curves. Adsorption mode and corrosion inhibition mechanism at different inhibitor concentrations on the steel surface were discussed. Soil simulating solution has been chosen a most corrosive soil composition. The selection criterion was mainly the chlorides and sulphates contents. Polyphosphates ions were selected as corrosion inhibitors in consequence of their environmental properties efficacy in soil.

2. Materials and methods

2.1 Study material

C-Mn steels were used as the working electrode for all studies. Samples were obtained from pipe Sonatrach Algerian gas producer's society. Materials have been chosen of tubes posed on the GZ1 line in 1974 which corrosion pits were detected. Samples were cut by flame – cut from the pipes walls and the test coupons were then cut from these sections by wet sawing. The cutting process was chosen as it does not alter the microstructure and corrosion test at the coupon surface, due to its low heat input and the absence of mechanical damage by avoiding the zones affected thermically. Pre-treatment of steels samples surfaces was carried out by grinding with emery paper of 600- 1200 grit, rinsing with bidistilled water, and ultrasonic degreasing in ethanol and dried at room temperature before us. All tests have been performed at 30± 1°C.

Steel have been manufactured by controlled lamination and accelerated cooling (TMCP) method from a variety of materials including carbon steel and corrosion resistant alloys according to the (API) 5L specification covers grade X60 and others grades [4] with a specified chemical composition and mechanical parameters including: yield strength, tensile strength and toughness that pipe must comply with. Chemical composition is specified as maximum limits of four elements, ie carbon, manganese, phosphorus and sulphur. The refinement of ferritic grain size has been   obtained by different mechanisms of hardening and precipitation based on the dislocation movement that increases elasticity limit and   steel tenacity. Hall-Petch laws [2] have since been verified experimentally and explain the hardening induced by a reduction in the ferritic grain size. Elemental composition of the samples was determined by emission spectroscopy and casting probe (Table1). Measured values were compared to values quoted in the material test certificates. Composition and microstructure can vary significantly between pipes. These variations result in substantial differences in corrosion performances of pipeline steel in a corrosion regime.

Table 1 - Elemental composition of steel (content of %),   (a_i is the considered test)

Elements	C	Mn	Si	P	S	Cr	Ni	Cu	Mo	V	Al
a_1	0.21	1.52	0.19	0.012	0.003	0.16	0.15	0.15	0.16	0.05	0.022
a_2	0.19	1.59	0.10	0.016	0.008	0.15	0.07	0.07	0.08	0.02	0.024
a_3	0.09	1.40	0.08	0.017	0.003	0.09	0.09	0.08	0.07	0.006	0.005

Micrographic analysis has been done by scanning electronic microscopy (SEM). It showed a fine pearlitic-ferritic microstructure. C-Mn Steel chemical composition (table1) showed microallied steel with a low carbon percentage 0.16% giving to steel a better chemical resistance and the presence of manganese in strong concentration (1.5 %) and low sulphur content. Chemical composition and mechanical properties are in conformity with the API norm, but contents high sulphur which in the presence of manganese can lead to the formation of the manganese sulphides (MnS) inclusions which are not wished in the microstructure being able to generate the starting of a corrosion pit and its propagation.

2.2 Soil simulating solution

The corrosion is related to soil conditions in which the structures are buried. The techniques available to determine the aggressiveness of the site may included laboratory test based on a soil chemical analysis in a specific location [5]. Several soil samplings have been taken from various sites which we have been chosen the most aggressive composition. Soil extract   was prepared according to AFNOR French norm A–05.250 P.278. A mass of soil is taken then mixed with distilled water and analyzed by spectrophotometry microanalysis. The chemical composition of soil is given in table 2. The criterion of steel aggressiveness is principally the chloride, sulphate and bicarbonate content. Test solution is obtained by reconstitution of chemical composition of soil in a solution called " soil simulating solution"

Table 2 - Chemical composition of soils solution from various sites (S_i is the considered soil sites)

Sites	Mass (mg/L)					
	Ca^{2+}	Mg^{2+}	K^+	Cl^-	SO_4^{2-}	HCO_3^-
S_1	94.60	56	7.6	76.9	736	117
S_2	18.96	16.44	11.7	47.33	458.4	183
S_3	----	---	6	7.8	74	218
S_4	2.00	29.04	1.82	22.69	37.48	160

Finally, we have reconstituted the chemical composition of the soil in a solution called ''soil simulating solution (Table 3). However, the analysis should also include a concentration of sodium, potassium and calcium ions so that an ionic balance can be struck. We have chosen the S4 solution which presents a corrosive character with a parameter of conductivity 65.5ms/cm and a pH 8.8.

Table 3 - Chemical composition of soil simulating solution (g/L)

$CaSO_4$	$MgSO_4$	K_2SO_4	NaCl	Na_2SO_4	$NaHCO_3$
2.00	29.04	1.82	22.69	37.48	0.16

2.3 Corrosion tests

Potentiodynamic polarization and impedance spectroscopy (EIS) were carried out by means of potentiostat equipment type Potentiostat / Galvanostat PGP 201   and controlled with Tacussel corrosion analysis software (VoltaMaster 4) to follow and record

the polarization curves, using a glass cell   with a capacity of 500 ml. Polarisation measurements were obtained using a conventional three-electrode cell with a platinum counter electrode and a saturated calomel electrode (SCE) as reference. The working electrode (WE) was in the steel form of a disk with an exposed area of 1 cm^2. The potentiodynamic current–potential curves were recorded by changing the electrode potential from -1400 mV to - 400 mV with scanning rate of 1.66 mV/s. The polarization resistance measurements were performed by applying a controlled potential scan over a small range typically 15 mV with respect to Ecorr. The resulting current is linearly plotted against potential, the slope of this plot at Ecorr being the polarization resistance (R$_p$). All tests were performed in de-aerated solutions under continuously stirred conditions at constant temperature: 25, 45 and 55 ± 0.1 °C using a thermostat.

The following experimental data have been obtained by electrochemical measurements with polyphosphates ions as corrosion inhibitors such as disodic hydrogeno-phosphate. The inhibitors solutions have been obtained by dissolution in fresh distilled water to obtain different concentrations (10^{-3}, 10^{-2}, 10^{-1}, 5.10^{-1}M) which have been added to complete the study solution.

Inhibition efficiencies were determined from corrosion values calculated by the Tafel extrapolation method and fitting the curve to the polarization equation. The inhibition efficiency has been calculated using the relationship [6]:

$$E\% = \frac{U_0 - U}{U_0} \quad (1)$$

Where U is the corrosion measurement such as polarization resistance, corrosion current density, and charge transfer resistance in absence of corrosion inhibitor and U$_0$ is the corrosion measurement in presence of corrosion inhibitor

3. Results and discussions

3.1. Potentiodynamic polarization

The potentiodynamic polarization tests showed that the anodic and cathodic polarization curves are recorded on study steel in de-aerated soil simulating solution at various pH and temperatures that simulates conditions of pipe soil environment.

3.1.1 pH influence

Potentiodynamic anodic and cathodic polarization curves were carried out at 30±0.1 °C in the pH range 5.0 - 8.5 in absence of inhibitors after 1h of immersion are shown in figure 1. The polarization parameters values of (Icorr), corrosion potential (Ecorr), polarization resistance and cathodic and anodic Tafel slopes (bc), (ba) are given in table 4.
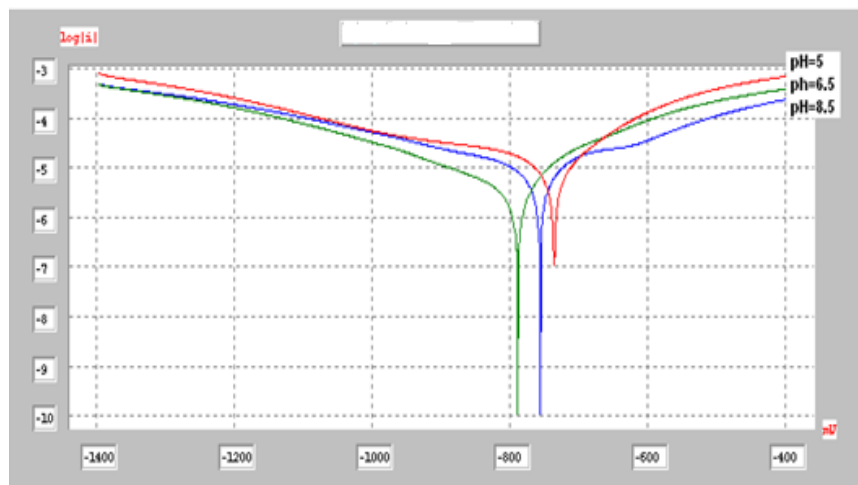
Figure 1 Potentiodynamic polarization curves for X60 steel in soil simulating solution at 30 °C.

The corrosion potential value (E$_{corr}$) is stabilizing after 1 hour and the low carbon steel corrosion in soil simulating solution is obtained. Polarization curves results showed that the corrosion of iron is a function of pH. If the pH values decrease toward the neutral or acidic pH in the range 5.0 – 8.5, steel corrosion increases and polarization resistance decreases. The potential corrosion tends towards the anodic values. In alkaline pH from pH ≈ 8.5 the steel corrosion decreases and the polarization resistance increases.

The pH   of soil will generally fall within the range 4 - 10. Soils containing well humified organic matter tend to be acidic. Mineral soils can become acidic due to leaching of basic cations (Ca^{2+}, Mg^{2+}, Na$^+$, and K$^+$) by rainwater and as the result of dissolving of carbon dioxide into the groundwater. In the context of steel corrosion in soil, the passivation occurs at high pH values. In contrast to iron, amphoteric metals which are protected by oxide films can be rapidly corroded in alkaline soils with high pH values as well as in acidic environments.

Table 4- Polarization parameters for the corrosion of X60 steel in Soil simulating solution according to the   pH variation   in the range   5.0 – 8.5

pH	E_{corr} (mV/SCE)	I_{corr} ($\mu A/cm^2$)	R_p ($k\Omega.cm^2$)	*Bc* (mV/dec)	*Ba* (mV/dec)
5.0	-740	7.5	6.2	-307	103
6.5	-793	7.4	7.5	-311	220
8.5	-760	4.8	10.6	-323	185

3.1.2 Effect of temperature

Polarisation measurements were taken at various temperatures in the absence of corrosion inhibitors in order to calculate the activation energies of the corrosion process. Polarization curves in the temperature range 25 – 55 °C at pH = 5 are shown in Figure 2. Polarization parameters values are given in table 5.
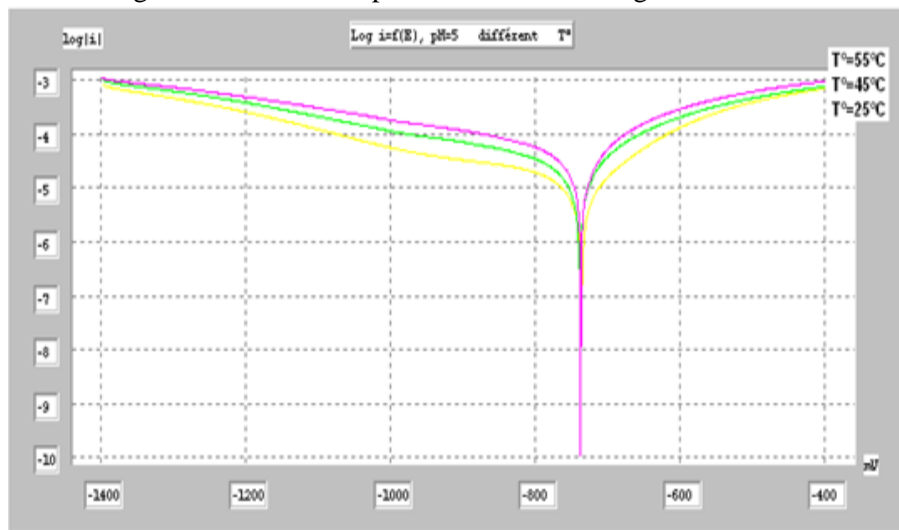
Figure 2 Potentiodynamic polarization curves for X60 steel in soil simulating solution at various temperatures (pH = 5)

Table 5- Polarization parameters for the corrosion of X60 steel in soil simulating solution according to the temperature   variation   in The range   25 – 55°C (pH = 5)

T (°C)	E_{corr}(mV/SCE)	I_{corr} ($\mu A/cm^2$)	R_p ($k\Omega.cm^2$)	*Bc* (mV/dec)	*Ba* (mV/dec)
25	-740	7.5	2.77	-307	103
45	-743	19.8	1.48	-239	125
55	-741	57.8	0.98	-342	213

In the studied temperature range, the corrosion current density increases with increasing temperature and the steel corrosion potential moves towards the negative values when the temperature increases in the studied solution. The anodic polarization curves present parallel Tafel straight lines indicating that the hydrogen reduction reaction to steel surface is always done according to activation mechanism in all the temperature range studied. In the industrial context, Gas pipelines operation shows that the temperature vary between seasons, or the climatic changes and can modify the interactions between steel and the middle environment in soil. In the temperature range at the near neutral pH, we have also a similar situation of electrochemical parameters variation. Polarization curves in the temperature range 25 – 55 °C at pH = 6.5 are shown in Figure 3. Polarization parameters values are given in table 6.

Polarization curves in the temperature range 25 – 55 °C at pH = 8.5 are shown in Figure 4. Polarization parameters values are given in table 7. The activation parameters for the corrosion process can be regarded as an Arrhenius-type process according to the following equation [7]:

$$\log I = -\frac{E_a}{2.303RT} + \log A \qquad (2)$$

And from transition state plot according to the following equation [5]:

$$\log \frac{I}{T} = -\frac{\Delta H^0_a}{2.303RT} + B \quad (3)$$

where E_a is the apparent activation energy, A the pre-exponential factor, R the universal gas constant, ΔH_a° the enthalpy of activation and T the absolute temperature. Figure 5 present the Arrhenius plots of corrosion current logarithm density vs. 1/T.
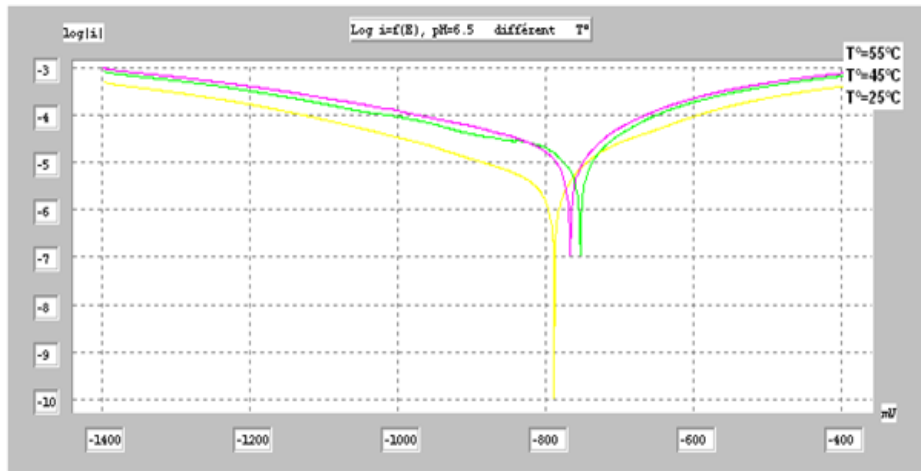
Figure 3 Potentiodynamic polarization curves for X60 steel in soil simulating solution at various temperatures (pH =6.5)

Table 6- Polarization parameters for the corrosion of X60 steel in soil simulating solution according to the temperature   variation   in The range   25 – 55°C (pH = 6.5)

Temperature (°C)	E_{corr} (mV/SCE)	I_{corr} (μA/cm^2)	R_p (kΩ.cm^2)	βc (mV/dec)	Ba (mV/dec)
25	-793	7.4	7.49	-311	177
45	-757	12	1.97	-331	162
55	-771	14	2.07	-337	195
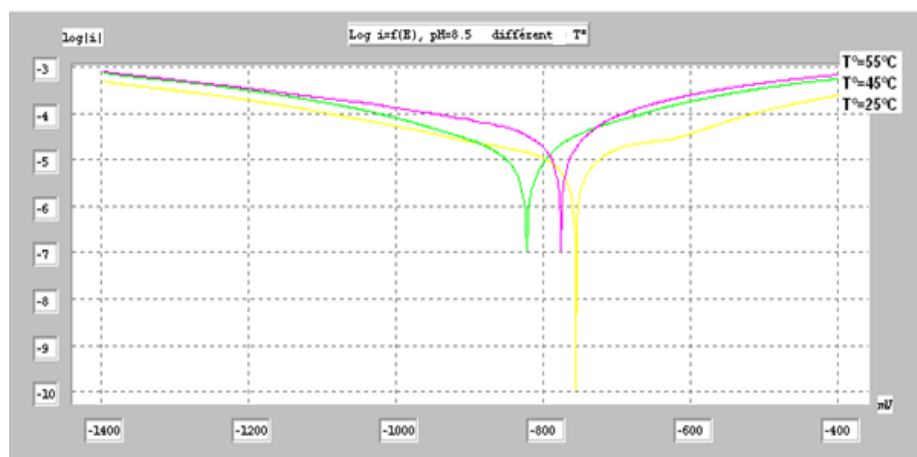
Figure 4 Potentiodynamic polarization curves for X60 steel in soil simulating solution at various temperatures (pH =8.5)

Table 7- Polarization parameters for the corrosion of X60 steel in soil simulating solution according to the temperature   variation   in The range   25 – 55°C (pH = 8.5)

Temperature (°C)	E_{corr} (mV/SCE)	I_{corr} (μA/cm^2)	R_p (kΩ.cm^2)	βc (mV/dec)	Ba (mV/dec)
25	-760	4.8	3.74	-323	184
45	-826	17.9	3.20	-285	225
55	-780	50.6	1.33	-160	268

Amara Zenati et al.
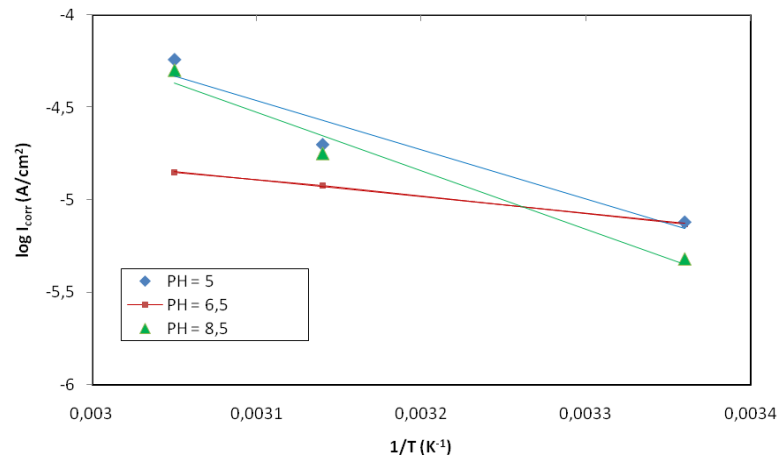
Figure 5 Arrhenius plot calculated from corrosion current density for X60 steel in soil simulating solution at different pH values

log (I/T) with reciprocal of the absolute temperature are presented in figure 6. Straight lines with coefficients of correlation close to 1 are obtained.
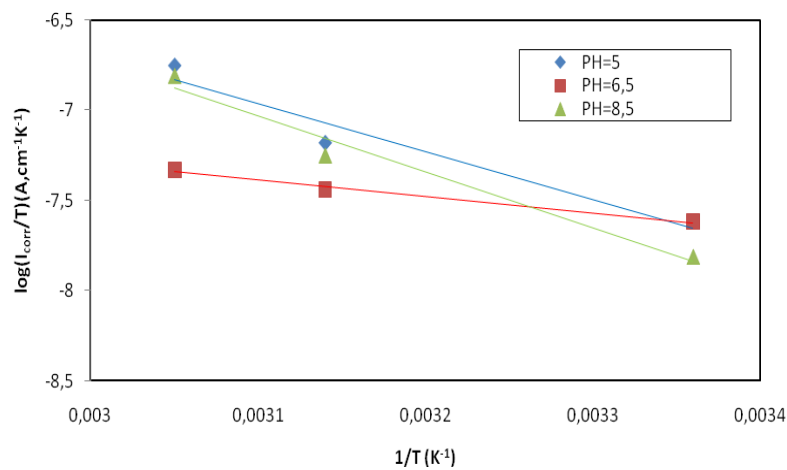
Figure 6 ln I_{corr} vs. $1/T$ for API steel dissolution in soil simulating at different pH.

The E_a energy values determined from the slopes of Arrhenius plots and are calculated to be $E_a = 17.48$ kJ mol^{-1}. This value is low compared to the value of steels corrosion activation energy in acidic environment [8,9] which to reach a value of 60 kJ mole[-1]. The activation energies values and delta H for different pH are gathered in table 8. The activation corrosion energy increases with the temperature according to the pH soil environment. These values are close to the literature except for the near neutral pH where the value is different.

Tableau 8- values of E_a and $\Delta H_a°$ for different pH

pH	E_a (kJ mole[-1])	$\Delta H_a°$ (kJ mole[-1])
5.0	51.01	49.18
6.5	17.48	14.48
8.5	59.22	58.15

3.2 Concentration influence
The electrochemical measurements have been obtained using the polyphosphates ions as corrosion inhibitors such as disodic hydrogeno-phosphate at various pH in range (5.0 - 8.5) and different concentrations which have been added to complete the study solution. For pH = 5.0, potentiodynamic anodic and cathodic polarization

curves were carried out at 30±0.1 °C in the absence and presence of inhibitors after 1h of immersion are shown in figure 7. The polarization parameters values of (I_{corr}), corrosion potential (E_{corr}), polarization resistance, cathodic and anodic Tafel slopes (βc), (βa) and the inhibition efficiency (E) are given in table 9.
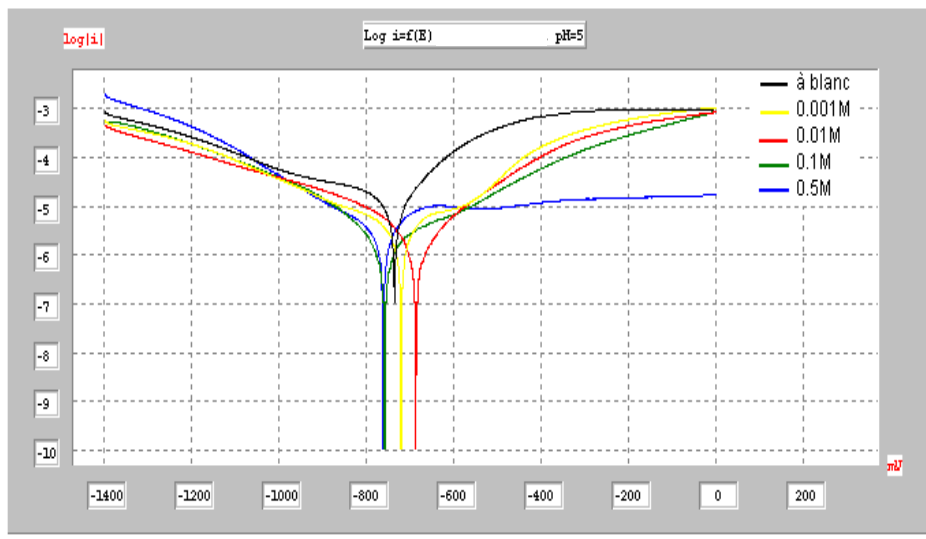
Figure 7 Potentiodynamic polarization curves for X60 steel in soil simulating solution at various concentrations of inhibitor (pH =5.0)

Table 9 Polarization parameters for the corrosion of X60 steel in Soil simulating solution according to the corrosion inhibitors concentration, (pH = 5.0)

Conc. (M)	E_{corr} (mV/SCE)	I_{corr} (μA/cm^2)	R_p (kΩ.cm^2)	Bc (mV/dec)	βa (mV/dec)	E% (I_{corr})	E% (R_p)
Blank	-740	7.5	6.2	-307	165	-----	----
10^{-3}	-725	4.6	11.2	-333	179	**38.7**	**44.9**
10^{-2}	-691	2.5	20.7	-373	173	**66.7**	**70.0**
10^{-1}	-763	2.1	23.8	-333	173	**72.0**	**73.9**
5.10^{-1}	-766	4.2	10.7	-213	204	**44.0**	**42.0**

For pH = 6.5 potentiodynamic anodic and cathodic polarization curves are shown in figure 8. The polarization parameters values and the inhibition efficiency (E) are given in table 10.
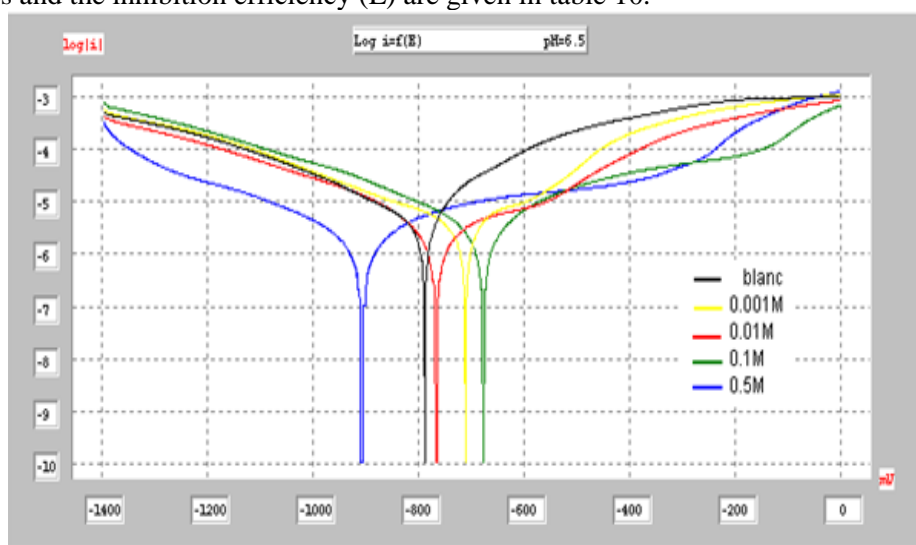
Figure 8 Potentiodynamic polarization curves for X60 steel in soil simulating solution at various concentrations of inhibitor (pH = 6.5)

Table 10 Polarization parameters for the corrosion of X60 steel in Soil simulating solution according to the corrosion inhibitors concentration (pH = 6.5)

Conc. (M)	E_{corr} (mV/SCE)	I_{corr} (μA/cm^2)	R_p (kΩ.cm^2)	Bc (mV/dec)	βa (mV/dec)	E% (I_{corr})	E% (R_p)
Blank	-793	6.5	7.5	-311	177	-----	----
10^{-3}	-715	5.2	10.5	-238	269	**20.0**	**28.5**
10^{-2}	-771	2.7	19.7	-355	187	**58.5**	**62.5**
10^{-1}	-682	2.2	16.1	-344	136	**66.1**	**53.4**
5.10^{-1}	-911	1.5	29.4	-309	152	**76.9**	**74.5**

For pH = 8.5 potentiodynamic anodic and cathodic polarization curves are shown in figure 9. The polarization parameters values and the inhibition efficiency (E) are given in table 11.
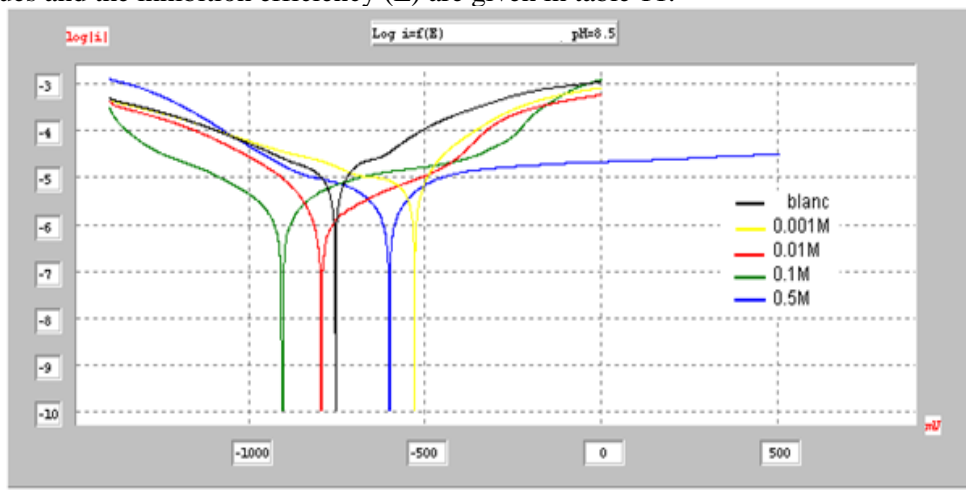
Figure 9. Potentiodynamic polarization curves for X60 steel in soil simulating solution at various concentrations of inhibitor (pH = 8.5)

Table 11 Polarization parameters for the corrosion of X60 steel in Soil simulating solution according to the corrosion inhibitors concentration (pH = 8.5)

Conc. (M)	E_{corr} (mV/SCE)	I_{corr} (μA/cm^2)	R_p (kΩ.cm^2)	Bc (mV/dec)	βa (mV/dec)	E% (I_{corr})	E% (R_p)
0	-760	4.8	10.5	-323	184	---	---
10^{-3}	-520	2.7	15.0	-232	157	**43.7**	**30.0**
10^{-2}	-800	1.6	32.1	-298	197	**66.7**	**67.3**
10^{-1}	-911	1.4	29.4	-282	152	**70.8**	**64.3**
5.10^{-1}	-608	2.0	19.6	-299	135	**58.3**	**46.3**

Results showed that, according to the concentration of inhibitor and the variation of pH in the range studied, the inhibition efficiency (E) is obtained for low value in acidic medium. We have obtained the similar situation when pH moved to basic near neutral value but decreases for 5.10^{-1}M.

3.3 *Adsorption consideration*

The interaction between the inhibitors and the API steel surface can be provided by the adsorption isotherm. In order to obtain the isotherm, the fractional coverage value θ as a function of inhibitor concentration must be obtained. The apparent corrosion rate of the inhibited steel electrode is proportional to the ratio of the surface covered θ and that not covered $(1- \theta)$ by the inhibitor. Fractional coverage values θ have been evaluated for different concentrations of the compound under study from corrosion rates in uninhibited and inhibited solutions by means of the equation:

$$\theta = \frac{I_u - I_i}{I_u} \qquad (4)$$

where I_u and I_i are the corrosion rate values without and with inhibitor, respectively.

The θ values for different inhibitor concentrations at different pH were tested by fitting to various isotherms. By far the best fit was obtained with the Langmiur isotherm. According to this isotherm θ is related to concentration inhibitor C via eq. 5:

$$\frac{C}{\theta} = \frac{1}{K} + C \quad \text{with} \quad K = \frac{1}{55,5}\exp(-\frac{\Delta G^0_{ads}}{RT}) \tag{5}$$

Where K is the adsorptive equilibrium constant and ΔG°_{ads} the free energy of adsorption.
Langmuir's plot for corrosion inhibition data of the compounds under investigation is showing in figure 10.
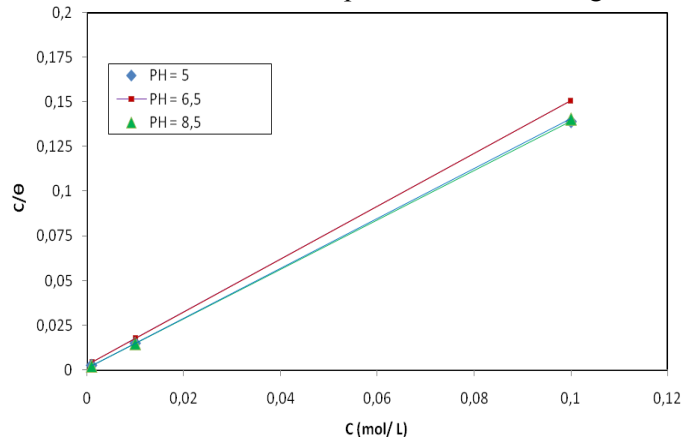
Figure 10 Curves fitting of the corrosion data of API steel in the presence of inhibitor to Langmuir isotherm.

Linear plots were obtained for inhibitor. These results suggest that the adsorption phenomenon obeys a modified Langmuir isotherm proposed by Villamil et al. [10], which is given by the corrected equation:

$$\frac{C}{\theta} = \frac{n}{K} + nC \tag{6}$$

Thermodynamic parameters are important to study the inhibitive mechanism. The values of ΔG°_{ads} at different pH were estimated from the values of K and equation (5).
The obtained values of K, n and ΔG°_{ads} are summarized in table 12.

Table 12. The thermodynamic parameters for of API steel in simulated soil solution in the absence and presence of different concentrations of the inhibitor.

pH	K (L/mol)	n	$-\Delta G^\circ_{ads}$ (kJ/ mol)
5	512.11	1.48	25.41
6.5	1131.15	1.38	27.37
8.5	1574.8	1.40	28.19

It can be seen that the values of the energy of adsorption are between -25.41 and -28.19 kJ/mol. The large negative of ΔG°_{ads} indicates that the inhibitor is strongly adsorbed on the steel surface [11]. It is well known that values of ΔG°_{ads} of the order of -20 kJ/ mol or lower indicate a physisorption, those of order of -40 kJ /mol orr higher involve charge sharing or a transfer from the inhibitor molecules to the metal surface to form a co-ordinate type of bond [12-13]. On the other hand, Metikos-Hukovic et al. [14] describe the interaction between thiourea and iron (ΔG°_{ads} = -39 kJ /mol) as chemisorptions [15]. Moreover, Bayoumi and Ghanem consider that the adsorption of naphthalene disulphonic acid on the mild steel was principally by chemisorptions (ΔG°_{ads} =-28.47 kJ /mol [16]. Thus, the ΔG°_{ads} value obtained here shows that in the presence of simulated soil solution, with a tendency to physisriroption of the inhibtitor on the API steel may occur.

Conclusion
Study steel is a low carbon steel and possessed an important corrosion rates in soil simulating solution test containing chlorides, phosphates and carbonates ions, which constitutes the natural environment often confronted in oil and gas prospection and transportation areas. The main objective of the present investigation was to study the susceptibility interactions of steel with the soil environment. Corrosion phenomena was simulated in laboratory while approaching the industrial context and chosen a most corrosive composition of soil simulating

solution. Appropriate models for corrosion parameters such as corrosion current density (I_{corr}), corrosion potential (E_{corr}), polarization resistance (R_p) are used to fit the experimental data and extract the parameters which characterize the corrosion process.

Results showed that if pH decreases in the pH range 5.0 - 8.5, steel corrosion increases and polarization resistance decreases. In the studied temperature range $25 – 55°C$, the corrosion current density increases with increasing temperature and the steel corrosion potential moves towards the negative values when the temperature increases

The activation corrosion energy increases with the temperature according to the pH soil environment. These values are close to the literature except for the near neutral pH where the value is different. Potentiodynamic polarization study with addition of the polyphosphates ions as corrosion inhibitors at various pH in range (5.0 - 8.5) in different low concentrations from 10^{-3} to 10^{-1} showed that the inhibition efficiency (E) is obtained for low value in acidic medium. We have obtained the similar situation when pH moved to basic near neutral value but decreases for the concentration of 5.10^{-1}M. The maximum inhibition efficiency was 75%. It has been obtained good agreement by calculation using different techniques. These results suggest that the adsorption phenomenon obeys a modified Langmuir isotherm. A future work will consist of using materials containing biomaterials as corrosion inhibitor where their effect on the environment is efficient, it is in progress.

References

1. Benmoussat A. and Hadjel M., *Eurasian Chem. Tech. Journal,* **7** (2) (2005) 147 – 156
2. Benmoussat A., Hadjel M. and Traisnel M., *Materials and Corrosion*, 57 (10) (2006) 771- 777.
3. Benmoussat A. and Traisnel M., Integrity of Pipelines Transporting Hydrocarbons, NATO Science for Peace and Security Series C: Environmental Security, (2011), pp 167-181.
4. API specification 5L (SPEC 5L), specification for line pipe, 14th edition, November 1, 1992, American petroleum institute 1220 L street, northwest Washington, DC 20005
5. Belmokre K., Azzouz N., Kermiche F., Wery M. and Pagetti J., Materials *and Corrosion*, 49 (1998) 108-113.
6. Landolt D., Corrosion Metals Surface Chemistry, *Alden Press, Oxford*, 1993, p. 495.
7. El Ouali I., Hammouti B., Aouniti A., Ramli Y., Azougagh M., Essassi E.M., Bouachrine M., *J. Mater. Environ. Sci.* 1 (2010) 1.
8. Larabi L., Harek Y., Benali O.and Ghalem S., *Progress in Organic Coatings*, 54 (2005) 256–262
9. Selles C., Benali B O., Tabti, Larabi L., Harek Y., *Mater J. Environ. Sci.*, 3 (1) (2012) 206-219.
10. Villamil R.F.V., Corio P., Rubin J.C., Agostinho S.M.L., *Electroanal J. Chem,* 535 (2002) 75-83
11. Fouda A.E., Mostafa H.A., Abu-Elnader H.M., Monatshefte fur Chem-104 (1989) 501.
12. Donahue F.M., Nobe K*., Electrochem J. Soc*. 112 (9) (1965) 886-891.
13. Khamis E., Bellucci F., Latanision R.M., El-Ashry E.S.H. *Corrosion* 47 (1991) 677-686.
14. Metikoš-Hukovič M., Babić R., Grubač Z., Brinić S., *J. Appl Electrochem*. 26 (1996) 443-449.
15. Benali O., Larabi L., Traisnel M., Gengembre L., Harek Y., *Appl. Surf. Sci*., 253 (2007) 6130–6139.
16. Ismail, A.I.M.; El-Shamy *Appl. Clay Sci.* 42 (2009) 356-362

(2014) ; http://www.jmaterenvironsci.com